

XAF690779
XA9640914

IC/95/357

**INTERNATIONAL CENTRE FOR
THEORETICAL PHYSICS**

**LOCAL COORDINATION AND MEDIUM RANGE
ORDER IN MOLTEN TRIVALENT METAL
CHLORIDES:
THE ROLE OF SCREENING
BY THE CHLORINE COMPONENT**



**INTERNATIONAL
ATOMIC ENERGY
AGENCY**



**UNITED NATIONS
EDUCATIONAL,
SCIENTIFIC
AND CULTURAL
ORGANIZATION**

G. Pastore

H. Tatlipinar

and

M.P. Tosi

MIRAMARE-TRIESTE

VOL 27 No 08

International Atomic Energy Agency
and
United Nations Educational Scientific and Cultural Organization
INTERNATIONAL CENTRE FOR THEORETICAL PHYSICS

**LOCAL COORDINATION AND MEDIUM RANGE ORDER
IN MOLTEN TRIVALENT METAL CHLORIDES:
THE ROLE OF SCREENING BY THE CHLORINE COMPONENT**

G. Pastore
Istituto Nazionale di Fisica della Materia and Dipartimento di Fisica Teorica,
Università di Trieste, Trieste, Italy,

H. Tatlipinar
International Centre for Theoretical Physics, Trieste, Italy
and
Department of Physics, Yildiz Technical University, 80270 Istanbul, Turkey
and

M.P. Tosi
Istituto Nazionale di Fisica della Materia and Classe di Scienze,
Scuola Normale Superiore, I-56126 Pisa, Italy.

Earlier work has identified the metal ion size R_M as a relevant parameter in determining the evolution of the liquid structure of trivalent metal chlorides across the series from $LaCl_3$ ($R_M \approx 1.4 \text{ \AA}$) to $AlCl_3$ ($R_M \approx 0.8 \text{ \AA}$). Here we highlight the structural role of the chlorines by contrasting the structure of fully equilibrated melts with that of disordered systems obtained by quenching the chlorine component. Main attention is given to how the suppression of screening of the polyvalent ions by the chlorines changes trends in the local liquid structure (first neighbour coordination and partial radial distribution functions) and in the intermediate range order (first sharp diffraction peak in the partial structure factors). The main microscopic consequences of structural quenching of the chlorine component are a reduction in short range order and an enhancement of intermediate range order in the metal ion component, as well as the suppression of a tendency to molecular-type states at the lower end of the range of R_M .

1. INTRODUCTION

A number of experimental studies have been reported in recent years on molten trivalent metal halides, with main attention to chlorides (for a review see Tosi, Price and Saboungi¹). The following trends in melting mechanism and liquid structure have been highlighted from diffraction experiments and a variety of other data:

(i) lanthanide metal trichlorides crystallizing in the typically ionic UCl_3 structure, such as $LaCl_3$, $PrCl_3$, $NdCl_3$ and $GdCl_3$, melt with an appreciable volume change into fully ionized liquids showing approximately eightfold first-neighbour coordination of the metal ions;²

(ii) YCl_3 and probably $DyCl_3$ melt with a very small volume change from the layer-type $AlCl_3$ structure into a liquid showing octahedral-type coordination and some amount of intermediate range order;³

(iii) $AlCl_3$ melts with very large volume and entropy changes from the same layer structure into a fourfold-coordinated liquid of strongly correlated molecular dimers⁴ or at least a fourfold-coordinated "sparse network liquid".⁵

The radius R_M of the metal ion in these compounds varies from about 1.4 Å for La^{3+} to about 1.2 Å for Y^{3+} and 0.8 Å for Al^{3+} . The above mentioned structural trends have been reproduced by means of a simple ionic model⁶ in correlation with R_M and with the number density of the melt. In essence, with decreasing R_M at constant density and temperature the model predicts increasing stability and decreasing coordination in the first neighbour shell of the metal ions, ending in a long-lived fourfold coordination in correspondence to compressed $AlCl_3$ at high density. This evolution in the local liquid structure parallels the growth of connectivity of the melt over increasing distances, leading to intermediate-range order and to the attendant first sharp diffraction peak (FSDP) in the diffraction patterns. Decreasing the number density then favours the formation of molecular states with strong intermolecular correlations.

Evidently the above summary account places main emphasis on structural aspects connected with the trivalent cations, while the role of the chlorine component in the melt is left implicit and apparently is merely to screen the strong Coulomb repulsions between the cations. However, the description of the crystalline structures of these compounds⁷ puts more emphasis on the chlorine

component. Thus, the ninefold-coordinated UCl_3 structure of $LaCl_3$ can be built by stacking into chains UCl_3 units shaped as trigonal pyramids and then packing the chains so as to give six intrachain and three coplanar interchain bonds to each metal ion. The $AlCl_3$ structure of YCl_3 and $AlCl_3$ can be built by arranging in layers the same basic pyramidal units and by packing the layers into a slightly distorted cubic close packing of chlorines, inside which the metal ions occupy planes of octahedral sites. While octahedral-type coordination is preserved in YCl_3 on melting,³ the melting of $AlCl_3$ can be viewed as accompanied by a cooperative transition of the metal ions from octahedral-type to tetrahedral-type coordination.⁴

In this work we discuss the consequences of taking a similar viewpoint on the microscopic structure of these compounds in disordered states. We contrast their structure in the melt at equilibrium with that of a partly quenched disordered medium. This is realized by having the cations permeate the micropores in a preformed disordered chlorine matrix, which is not allowed to relax itself to equilibrium so as to screen the cation-cation Coulomb repulsions. Recent developments in the statistical mechanics of disordered systems⁸⁻¹⁷ allow one to map such a problem into a classical liquid-structure problem. A preliminary report on the results that we present below has already appeared in the literature.¹⁸

2. METHOD

As in our earlier work on fully annealed trichloride melts⁶ (hereafter referred to as D), we use the hypernetted chain closure

$$g_{ij}(r) = \exp[-\beta\Phi_{ij}(r) + h_{ij}(r) - c_{ij}(r)] \quad (2.1)$$

to relate the partial pair distribution functions $g_{ij}(r) = h_{ij}(r) + 1$ to the interionic pair potentials $\Phi_{ij}(r)$ and to the partial Ornstein-Zernike functions $c_{ij}(r)$. Here we use the suffixes $i = 1$ for the Cl^- component and $i = 2$ for the trivalent metal component and denote by n_i their partial mean densities.

The disordered chlorine matrix is realized by combining eqn (2.1) for $g_{11}(r)$ with the Ornstein-Zernike relation for a one-component disordered medium. After taking Fourier transforms this is

$$h_{11}(k) = c_{11}(k) + n_1 c_{11}(k) h_{11}(k) \quad (2.2)$$

The corresponding equations for the metal ions permeating the chlorine matrix are taken from the work of Madden and Glandt,⁸

$$h_{12}(k) = c_{12}(k) [1 - n_2 c_{22}(k)]^{-1} + n_1 c_{11}(k) h_{12}(k) \quad (2.3)$$

and

$$h_{22}(k) = c_{22}(k) + n_1 c_{12}(k) h_{12}(k) + n_2 c_{22}(k) h_{22}(k) \quad (2.4)$$

These describe an annealed fluid which has reached equilibrium with the fixed distribution of potentials generated by the quenched matrix. Equations (2.2) - (2.4) should be compared with the well known Ornstein-Zernike relations for a fully annealed two-component fluid:

$$h_{ij}(k) = c_{ij}(k) + n_1 c_{i1}(k) h_{1j}(k) + n_2 c_{i2}(k) h_{2j}(k) \quad (2.5)$$

The above equations have been solved numerically by means of the Gillan-Abernethy algorithm^{21,22} on a discrete mesh of 513 points with a spacing $\delta r = 0.05a$, a being the ion-sphere radius. We have checked for YCl_3 at high temperature that the set of Ornstein-Zernike relations derived by Given and Swell^{12,13} for a partly quenched disordered system yield practically the same results as the simpler relations reported in eqns (2.2) - (2.4). This parallels our earlier findings for partly quenched $CuCl$.²³ The Madden-Glandt relations allow a significant reduction in numerical effort and yield rapid convergence even at low temperature.

The pair potentials that we have adopted in our calculations are of the Busing type,¹⁹ consisting of Coulomb interactions between point-like integer ionic charges and of exponential overlap repulsions. The parameters were given in I from an analysis²⁰ of bond lengths and vibrational Raman frequencies of bound molecular-ion states formed by trivalent metal ions in liquid mixtures of their halides with alkali halides. Each ionic component is implicitly taken to be neutralized by a uniform inert background.

For a more direct assessment of the structural trends the temperature T and the number density n of formula units have been kept fixed at the values $T = 1020$ K and $n = 0.0316 \text{ \AA}^{-3}$. These values are appropriate to YCl_3 near melting, this compound lying near the middle of the range of R_M that we examine. Thus the results that we report in the following sections refer to an expanded state in the case of $LaCl_3$ and to a compressed state in the case of $AlCl_3$.

3. LOCAL STRUCTURE

Figure 1 reports the chlorine-chlorine radial distribution functions appropriate to our models for expanded $LaCl_3$ (E- $LaCl_3$), YCl_3 and compressed $AlCl_3$ (C- $AlCl_3$). Here and in the following figures, full curves refer to fully annealed melts and dashed curves to partly quenched systems.

The quenched chlorine structure in Figure 1 is quite close to a disordered close packing of almost hard spheres. Relative to this basic structural frame, the annealed melts show a contraction in the chlorine-chlorine bond length and secondary structures beyond close contact. The bond length contraction increases with decreasing R_M , thus making it clear that it is directly induced by the Coulomb attractions exerted on the chlorines by the trivalent cations. The secondary structures reflect adjustments of the chlorines at longer range and are especially noticeable in E- $LaCl_3$ where, as discussed further below, the main ordering arises from the Coulomb repulsions between the cations within an essentially loose ionic melt.

Figure 2 reports the running coordination number $N_{21}(r)$ of the cation by chlorines, which is defined as

$$N_{21}(r) = 4\pi n_1 \int_0^r dr' r'^2 g_{12}(r') \quad (3.1)$$

while Figure 3 shows the cation-chlorine radial distribution functions. In the partly quenched system the cations can evidently occupy only suitable pre-existing holes within the rigid chlorine frame. It is seen from Figure 2 that the cations in the quenched system succeed in preserving an average first-neighbour coordination number close to, but somewhat lower than, that of the annealed melt. This is of order 7 to 8 for La^{3+} in E- $LaCl_3$, of order 5 to 6 for Y^{3+} in YCl_3 and close to 4 for Al^{3+} in C- $AlCl_3$. The decrease in first-neighbour coordination becomes more noticeable as one moves from E- $LaCl_3$ to C- $AlCl_3$ and is also evident in Figure 3 from the decreased height of the main peak in $g_{12}(r)$. The parallel change in slope of the plateau in $N_{21}(r)$ in Figure 2 and the increased value of $g_{12}(r)$ at its main minimum in Figure 3 show that the reduction in coordination in YCl_3 and in C- $AlCl_3$ is accompanied by an increased freedom of exchange between first and second neighbour shells. In summary, within the rigid chlorine frame each type of cation preferentially samples holes providing its most appropriate coordination and

moves with greater freedom within its preferred subsystem of structural holes.

Finally, Figure 4 reports the cation-cation radial distribution functions. We recall from I that on reducing the density the double-peak structure shown in $g_{AlAl}(r)$ in the annealed C-AlCl₃ melt is resolved into two separate peaks with a total Al-Al coordination number approximately equal to unity. This trace of a tendency to formation of dimeric states is accompanied by persistence in a state of intermediate range order in the subsystem of the cations. At reduced density the model can be driven to an instability against liquid-vapour phase separation on reducing the temperature.

Major consequences of chlorine quenching are seen in Figure 4 to occur in YCl₃ and in C-AlCl₃. As we shall see more clearly in the next section from the corresponding partial structure factors, chlorine quenching induces in YCl₃ and C-AlCl₃ a major enhancement of the state of medium range order in the metal ion component. Correspondingly the main feature in the cation-cation radial distribution function which should be noticed in Figure 4 for these two systems in the partly quenched state is the nearly periodic sequence of peaks with a repeat distance approximately equal to 2.5 a.

4. INTERMEDIATE AND SHORT RANGE ORDER

Figure 5 compares the cation-cation structure factors for the three models in the annealed and partly quenched states. It is useful to recall at this point the interpretation that was given in I for the cation-cation correlations in the annealed melt, a crucial element being the relative location of the main features of the cation-cation structure factor on superposition to the cation-chlorine and chlorine-chlorine structure factors. Adopting the terminology which has come to be accepted in discussing the structure of melts of divalent cations such as SrCl₂ and ZnCl₂,³ the main peak in $S_{LAlA}(k)$ is best described as reflecting ordering from strong Coulomb repulsions between the cations in an essentially loose ionic melt, whereas the main peak in $S_{YY}(k)$ and in $S_{AlAl}(k)$ is interpreted as a marker of intermediate range ordering of the cations in a melt showing connectivity of strong local structures. In fact, a partly self-frustrating admixture of Coulomb order and medium range order is present in the annealed YCl₃ melt. In all cases the main peak in the cation-cation structure factor lies at $k \approx 2.5/a$. The second peak in $S_{YY}(k)$ and in $S_{AlAl}(k)$ is

instead in phase with the main peak in the chlorine-chlorine structure factor and with a trough in the cation-chlorine structure factor. It thus reflects the Coulomb alternation of the two ionic species.

It is seen from Figure 5 that quenching of the chlorines into a rigid disordered frame induces a major strengthening and sharpening of the main peak in the cation-cation structure factor. In all cases the cations establish their own state of internal order under their mutual Coulomb repulsions and in doing so take much better advantage of structural holes in the chlorine matrix when the latter is quenched. Of course, as we have already seen from Figure 2 such holes are preferentially of octahedral type in YCl₃ and of tetrahedral type in C-AlCl₃.

Figure 5 also shows that appreciable changes occur on chlorine quenching in $S_{YY}(k)$ and in $S_{AlAl}(k)$ at larger wave number. The behaviour shown for YCl₃ in Figure 5.b is best described as a reduction in order from Coulomb alternation induced by the enhancement in the intermediate range order. The most direct interpretation of the changes in short range ordering of the cations in C-AlCl₃ is instead offered by Figure 4.c above, showing that traces of a tendency to dimeric states are completely suppressed on chlorine quenching.

The cation-chlorine and chlorine-chlorine structure factors in the annealed YCl₃ and C-AlCl₃ melts show a peak at $k \approx 2.5/a$, which is a ghost of the intermediate range order in the cation subsystem. As illustrated in Figure 6 for C-AlCl₃, on chlorine quenching this feature is reduced in the cation-chlorine structure factor and is totally suppressed in $S_{ClCl}(k)$. In addition, $S_{AlCl}(k)$ in Figure 6.a shows some reduction in its main trough, which is the well known marker of Coulomb alternation between the two species in an ionic disordered system. This is, of course, the k-space counterpart of the structural changes that we have already seen in Figure 3.c above.

As a last comment we draw attention to the fact that all the partial structure factors in the partly quenched systems vanish in the limit $k \rightarrow 0$. Partial quenching suppresses all long-wavelength fluctuations of the partial ionic densities.

5. CONCLUDING REMARKS

We have reported the results of calculations on two types of disordered state for model

systems adjusted to simulate trivalent metal chlorides over a wide range of cation radius running from LaCl_3 to AlCl_3 . Quenching of the chlorines into a disordered matrix, by suppressing their screening of the Coulomb repulsions between the trivalent cations, emphasizes the structural features which are most direct consequences of these repulsions - i.e., primarily, the state of intermediate range order of the cations. In both the annealed melt and the partly quenched disordered system this state is achieved by the selective occupation of holes within the chlorine structure, the "preferred" subsystem of holes for each type of cation being determined by its ionic radius. In the partly quenched state, as a further consequence of suppressed screening, the diffusive motions of the cations are enhanced. This latter finding agrees with our earlier results for partly quenched CuCl .²³

Acknowledgements

One of us (HT) acknowledges support from the Bogaziçi University Centre for Turkish-Balkan Physics Research and Applications, from the Turkish Scientific and Technological Research Council (Tubitak) and from Yıldız Technical University.

References

1. M. P. Tosi, D. L. Price and M.-L. Saboungi, *Ann. Rev. Phys. Chem.*, **44**, 173 (1993).
2. J. Mochinaga, Y. Iwadata and K. Fukushima, *Mat. Sci. Forum*, **73**, 147 (1991).
3. M.-L. Saboungi, D. L. Price, C. Scamehorn and M. P. Tosi, *Europhys. Lett.*, **15**, 283 (1991).
4. N. H. March and M. P. Tosi, *Phys. Chem. Liquids*, **10**, 39 (1980), and references given therein.
5. Y. S. Badyal, D. A. Allen and R. A. Howe, *J. Phys.: Condens. Matter*, **6**, 10193 (1994).
6. H. Tatlipinar, Z. Akdeniz, G. Pastore and M. P. Tosi, *J. Phys.: Condens. Matter*, **4**, 8933 (1992).
7. R. W. G. Wyckoff, *Crystal Structures*, vol. 2 (Interscience, New York 1964), pp 45-77.
8. W. G. Madden and E. D. Glandt, *J. Stat. Phys.*, **51**, 537 (1988).
9. L. A. Fanti, E. D. Glandt and W. G. Madden, *J. Chem. Phys.*, **93**, 5945 (1990).
10. W. G. Madden, *J. Chem. Phys.*, **96**, 5422 (1992).
11. W. G. Madden, *J. Chem. Phys.*, **102**, 5573 (1995).
12. J. A. Given and G. Stell, *J. Chem. Phys.*, **97**, 4573 (1992).
13. J. A. Given and G. Stell, in *Condensed Matter Theories*, ed. L. Blum and F. Bary Malik (Plenum, New York 1993), p. 395.
14. E. Lomba, J. A. Given, G. Stell, J. J. Weis and D. Levesque, *Phys. Rev. E*, **48**, 233 (1993).
15. E. Pitard, M. L. Rosinberg, G. Stell and G. Tarjus, *Phys. Rev. Lett.*, **74**, 4361 (1995).
16. D. Chandler, *J. Phys.: Condens. Matter*, **3**, F1 (1991).
17. M. P. Tosi, *N. Cimento D*, **16**, 169 (1994).
18. H. Tatlipinar, G. Pastore and M. P. Tosi, *Phil. Mag. Lett.*, **68**, 357 (1993).
19. R. W. Busing, *Trans. Am. Crystallogr. Assoc.*, **6**, 57 (1970).
20. A. Erbölükbas, Z. Akdeniz and M. P. Tosi, *N. Cimento D*, **14**, 87 (1992).
21. M. J. Gillan, *Molec. Phys.*, **38**, 1781 (1979).
22. G. M. Abernethy and M. J. Gillan, *Molec. Phys.*, **39**, 839 (1980).
23. H. Tatlipinar, G. Pastore and M. P. Tosi, *Phys. Chem. Liquids*, in press.

Figure captions

Figure 1. The chlorine-chlorine pair distribution function of (a) expanded LaCl_3 , (b) YCl_3 and (c) compressed AlCl_3 in the annealed molten state (full curves) and in a chlorine-quenched state (dashed curves).

Figure 2. Running coordination number of a cation by chlorines in (a) expanded LaCl_3 , (b) YCl_3 and (c) compressed AlCl_3 . The curves are as in Figure 1.

Figure 3. Cation-chlorine pair distribution function in (a) expanded LaCl_3 , (b) YCl_3 and (c) compressed AlCl_3 . The curves are as in Figure 1.

Figure 4. Cation-cation pair distribution function in (a) expanded LaCl_3 , (b) YCl_3 and (c) compressed AlCl_3 . The curves are as in Figure 1.

Figure 5. Cation-cation partial structure factor in (a) expanded LaCl_3 , (b) YCl_3 and (c) compressed AlCl_3 . The curves are as in Figure 1.

Figure 6. Cation-chlorine (a) and chlorine-chlorine (b) partial structure factor in compressed AlCl_3 . The curves are as in Figure 1.

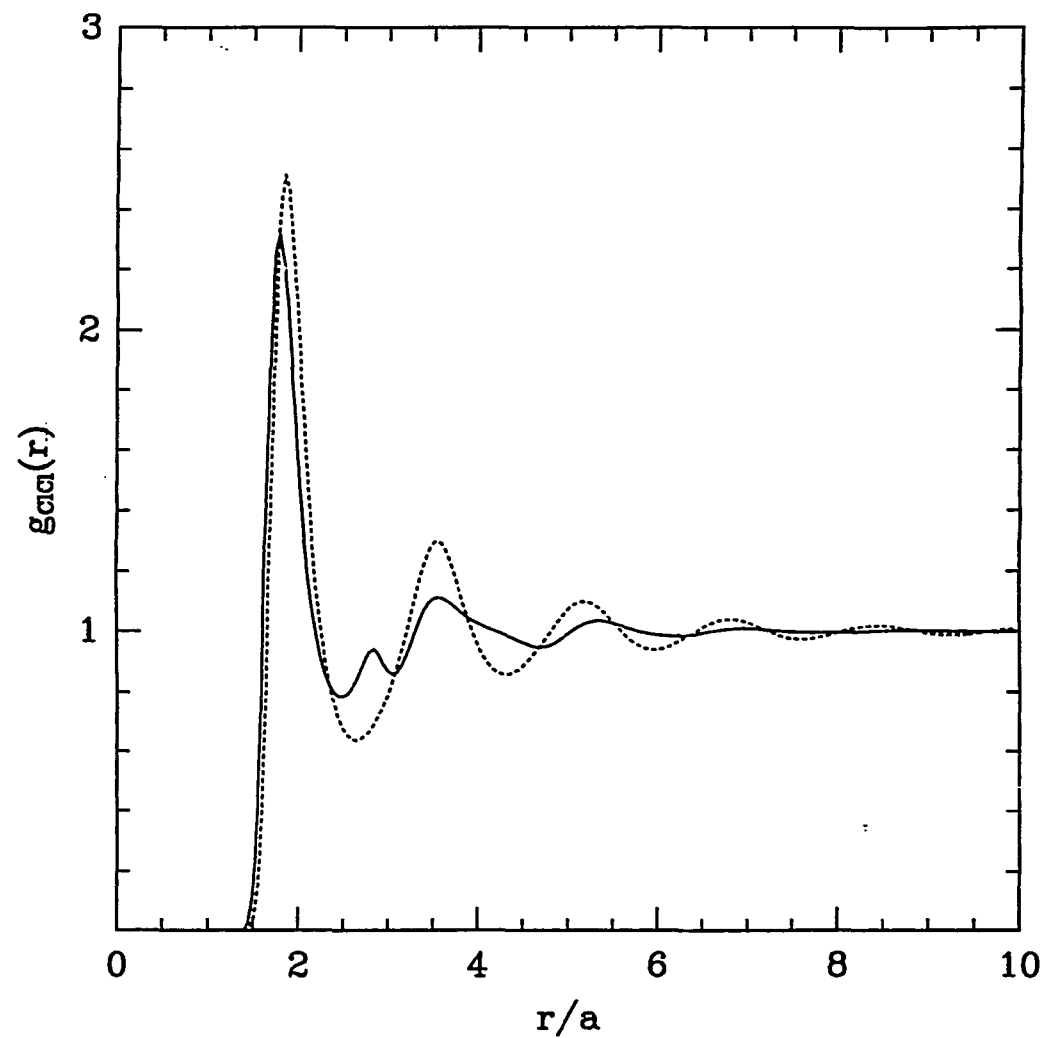


Fig. 1a

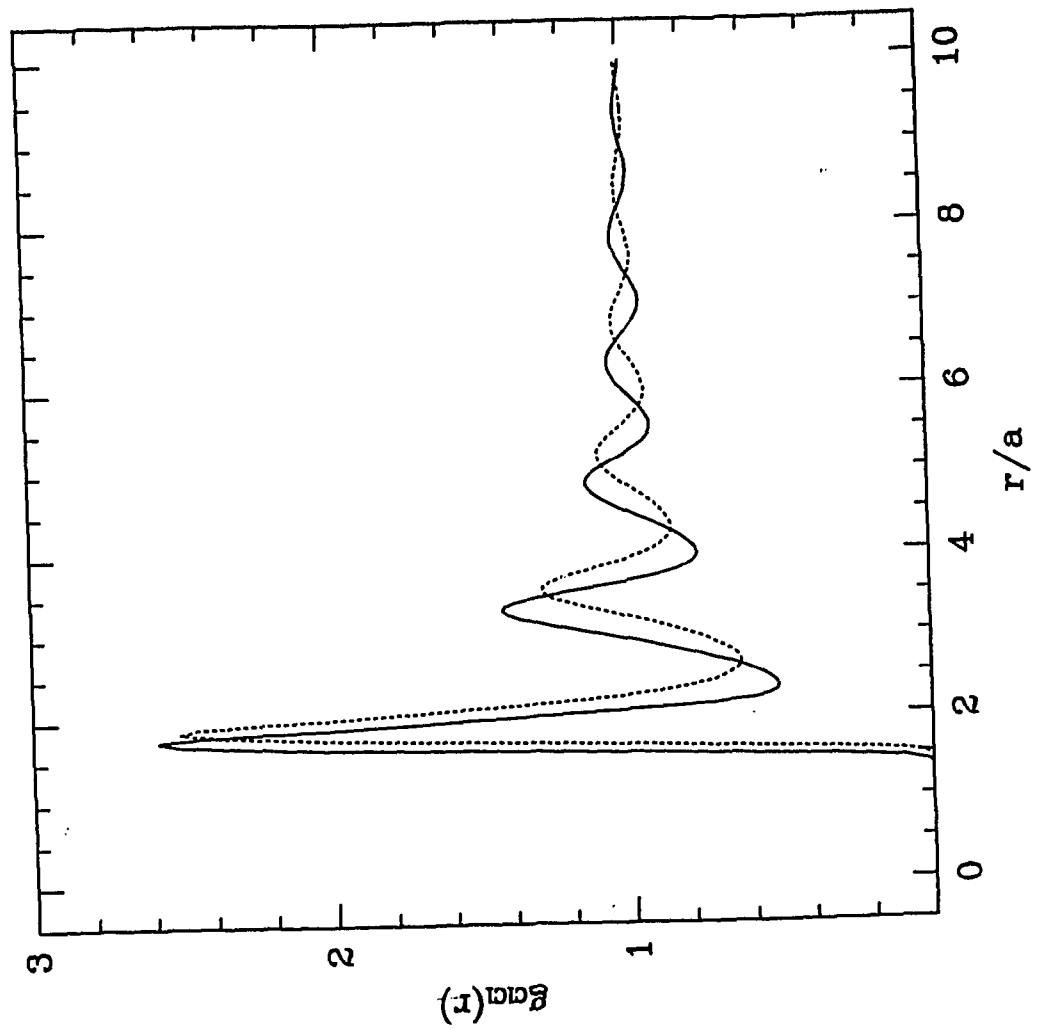


Fig. 1c

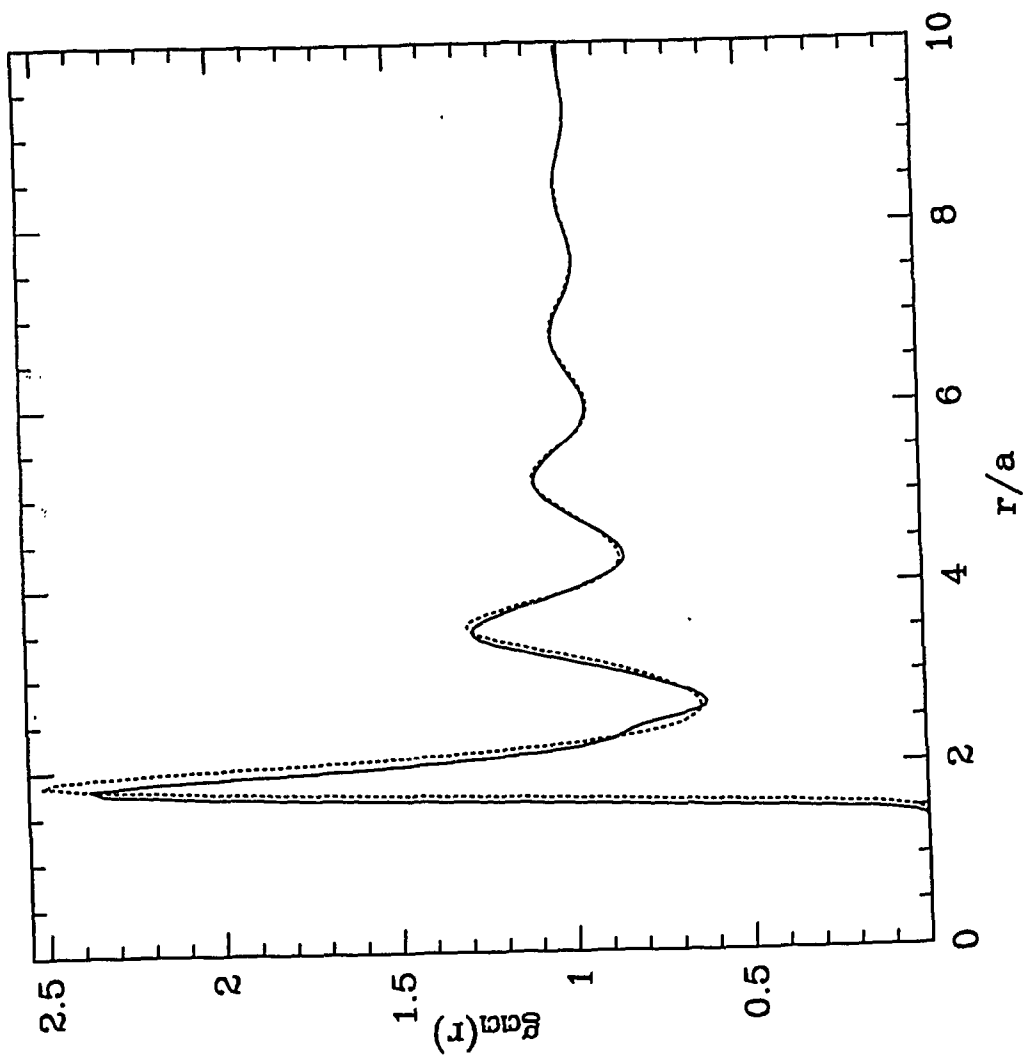


Fig. 1b

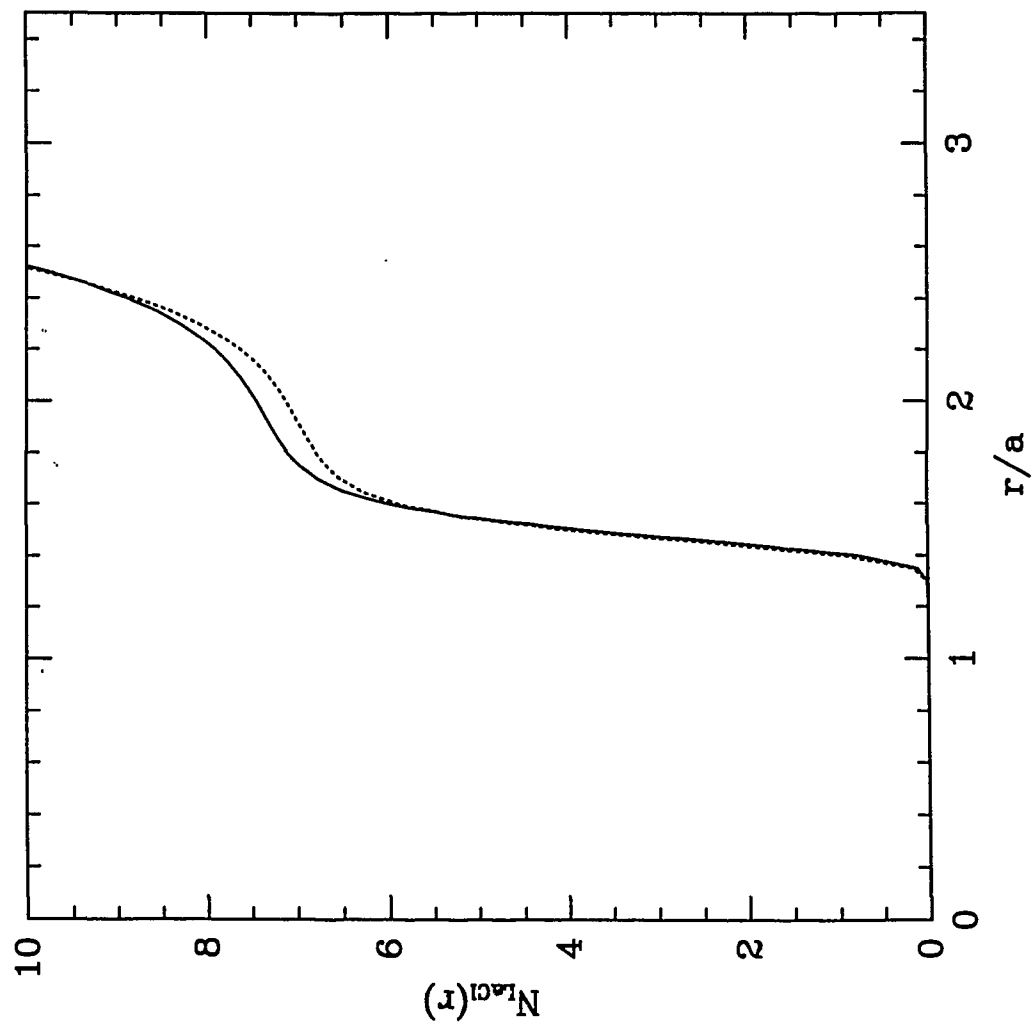


Fig. 2a

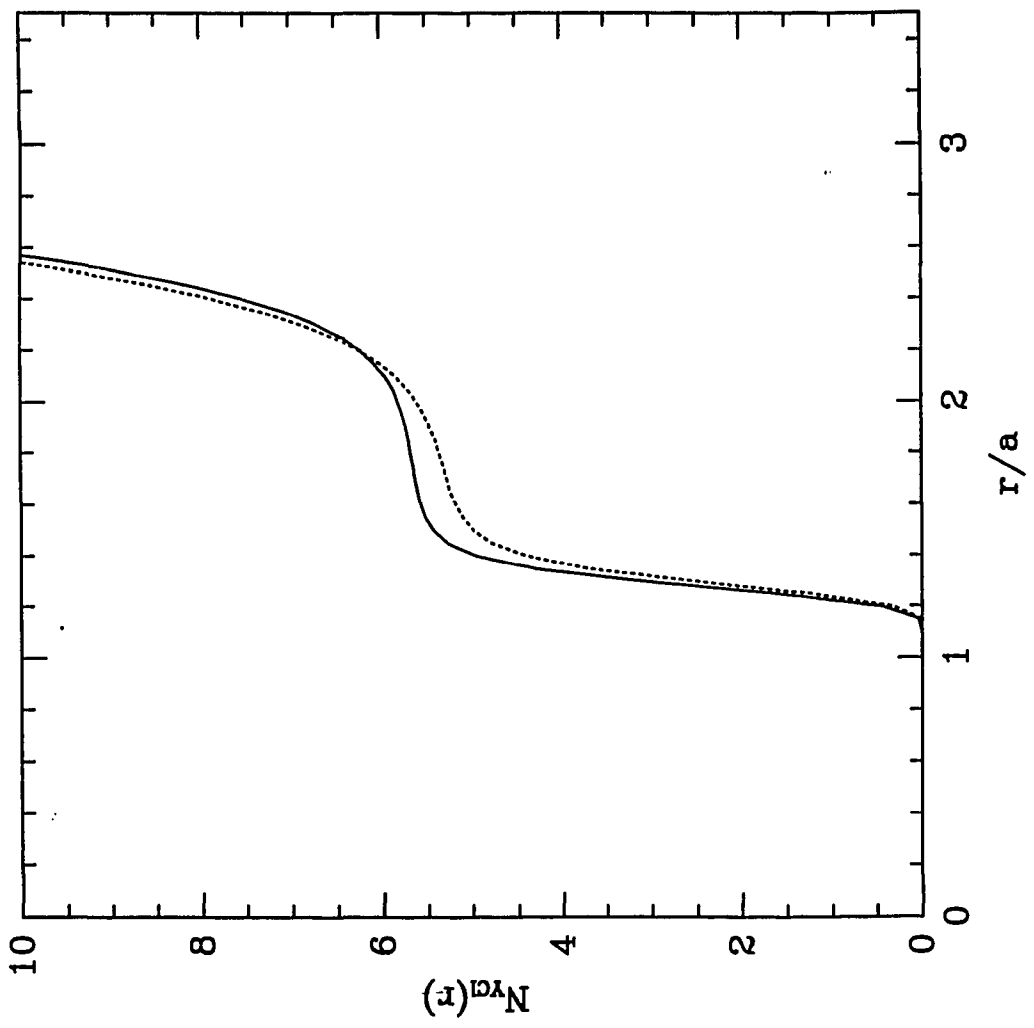


Fig. 2b

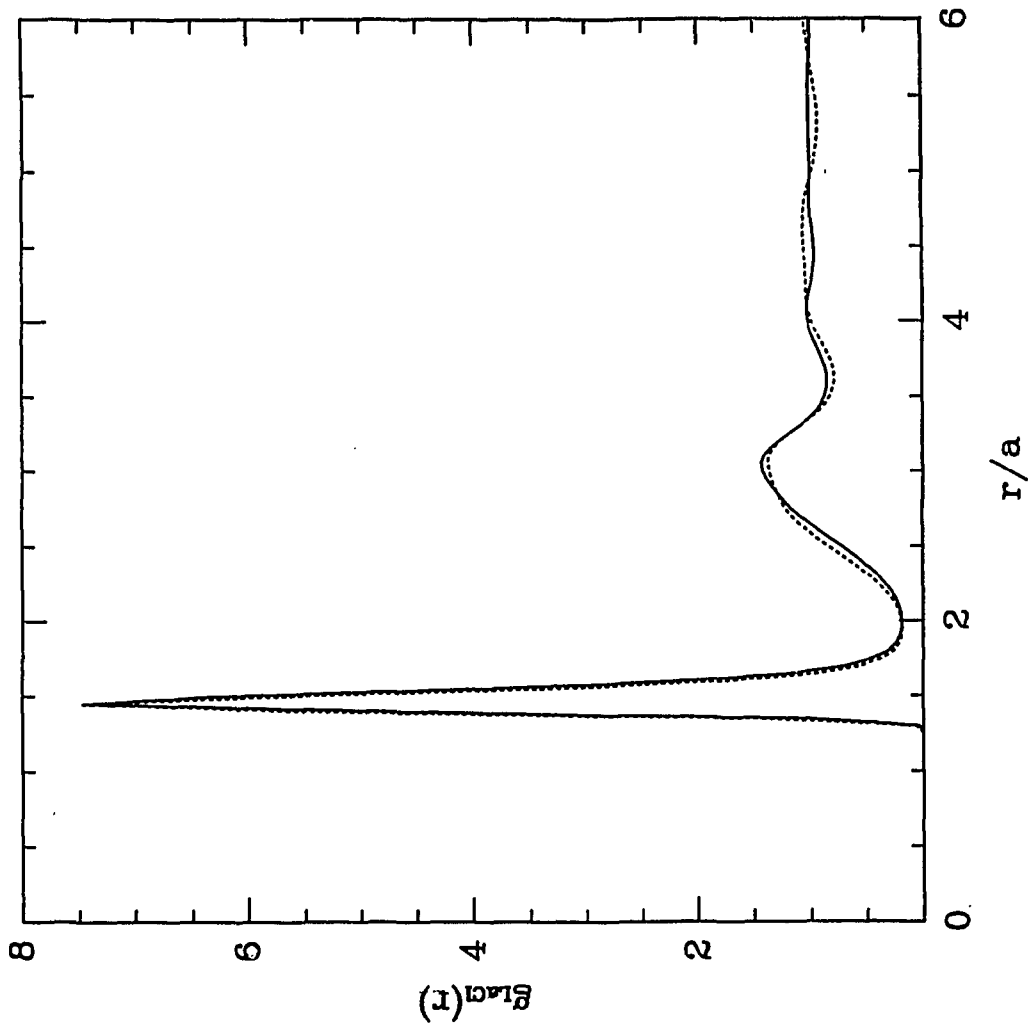


Fig.3a

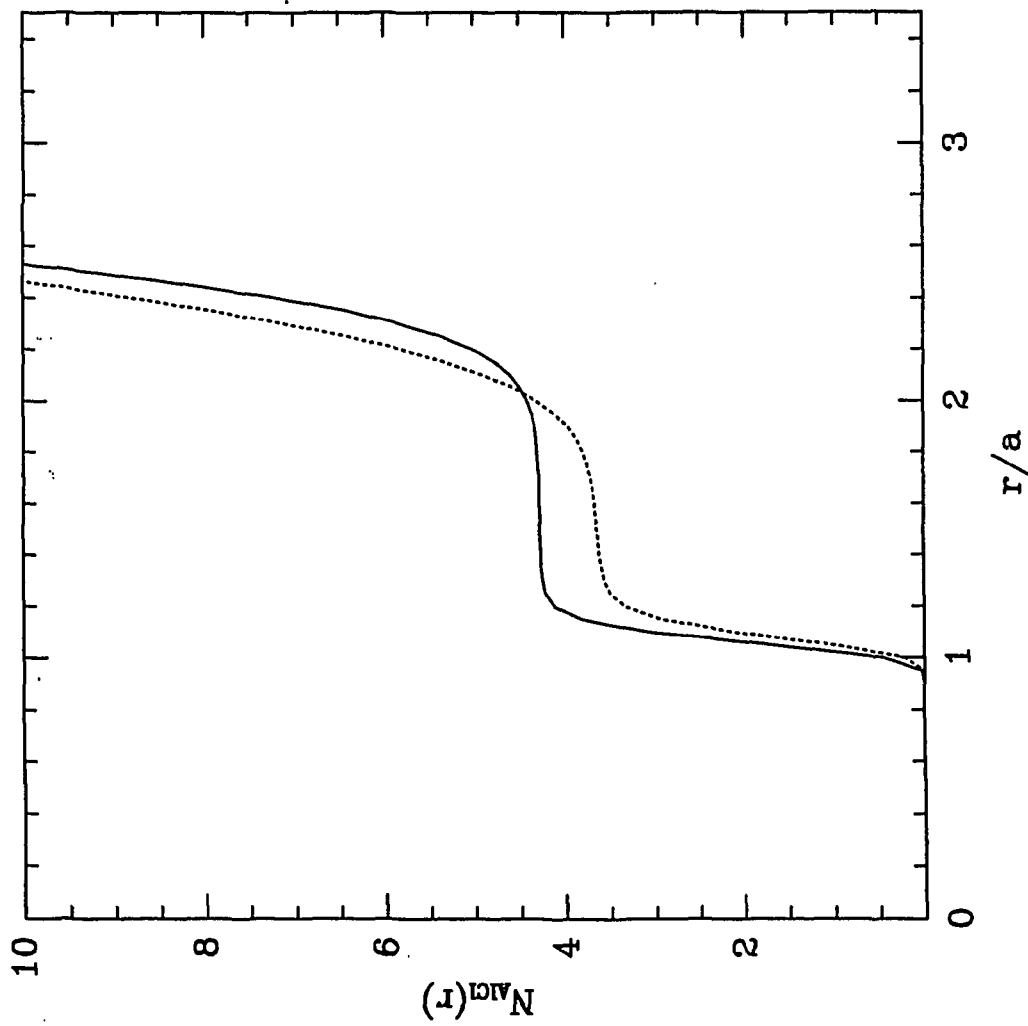


Fig.2c

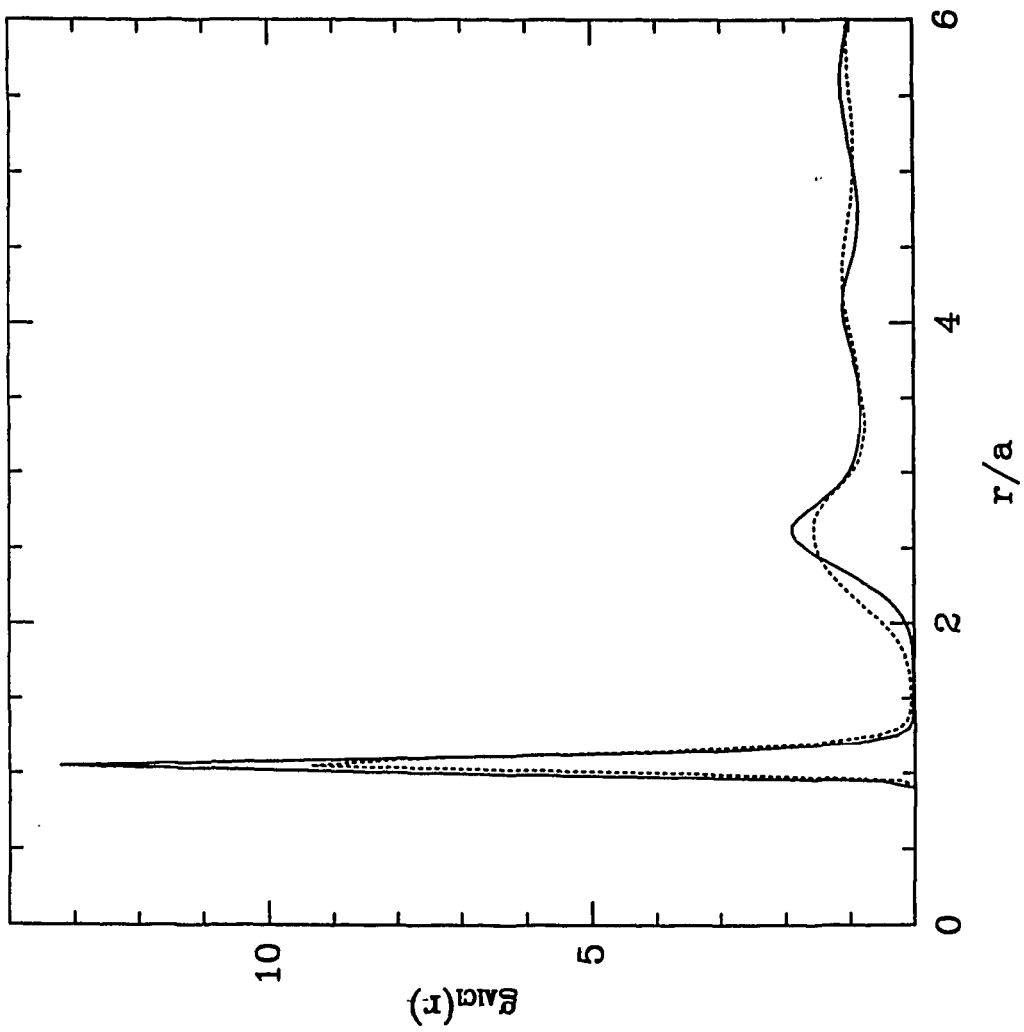


FIG. 3c

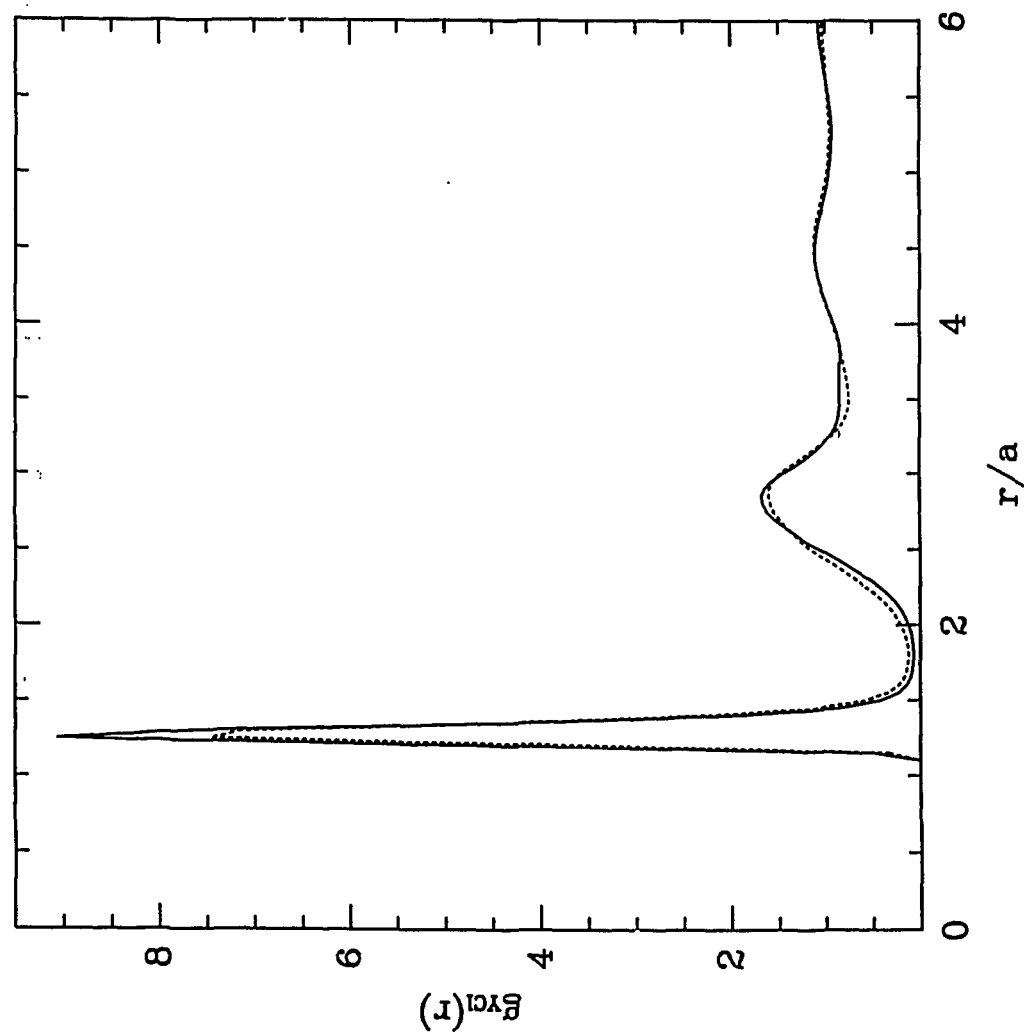


Fig. 3b

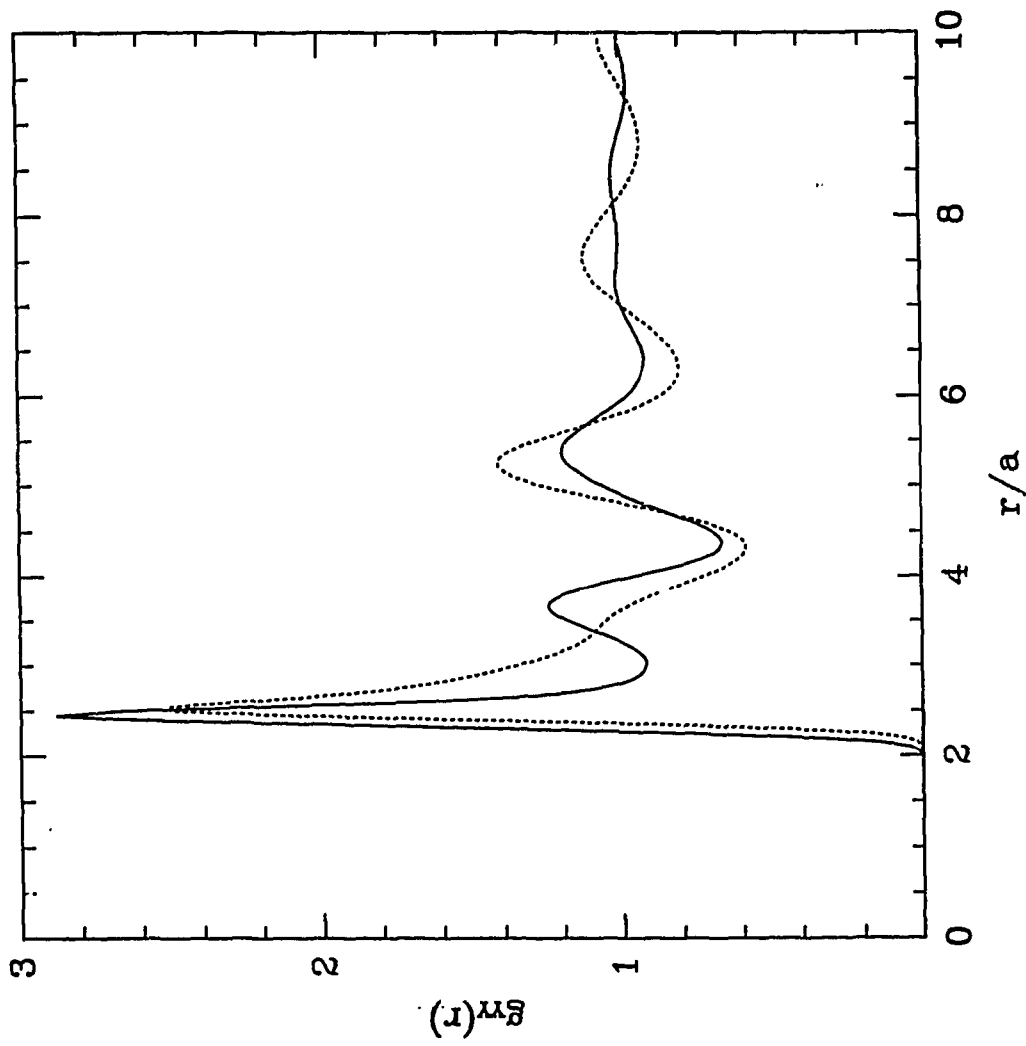


Fig.4a

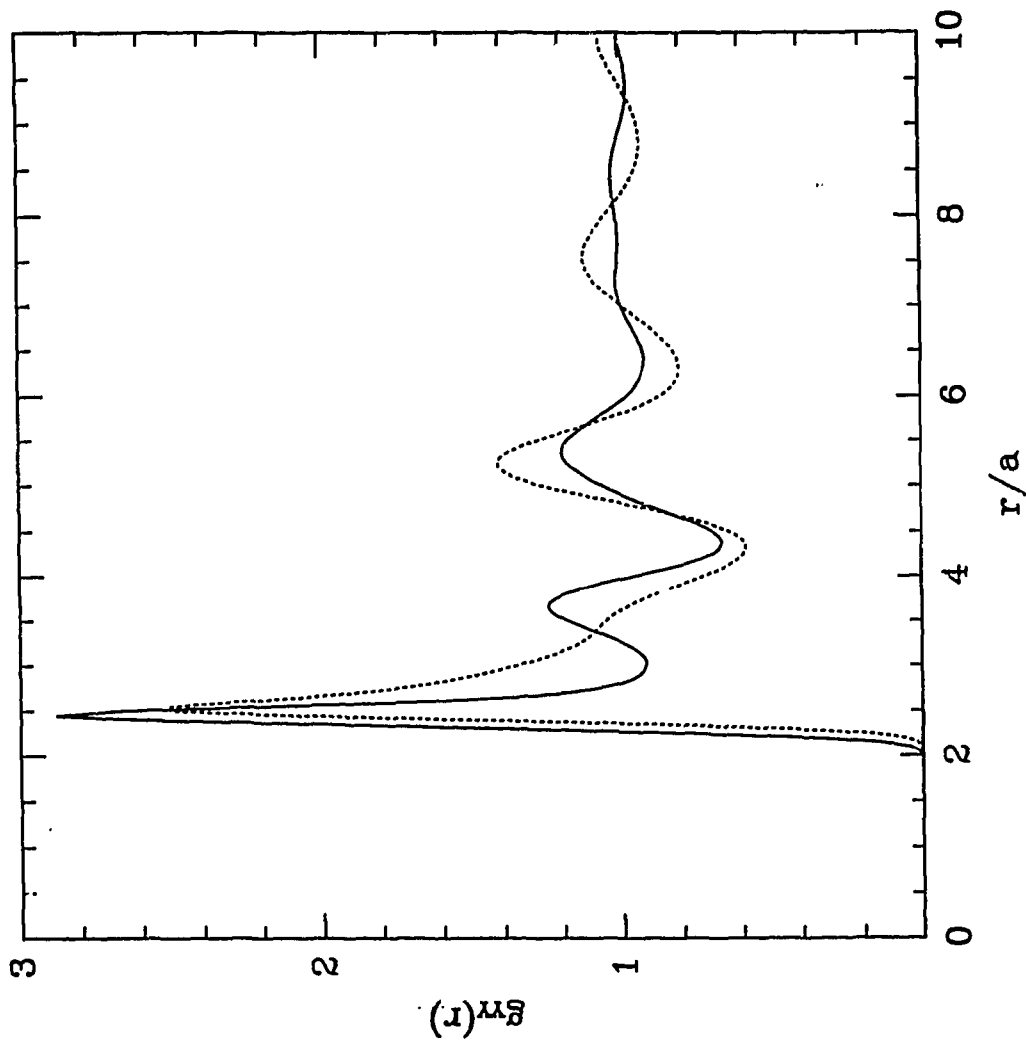


Fig.4b

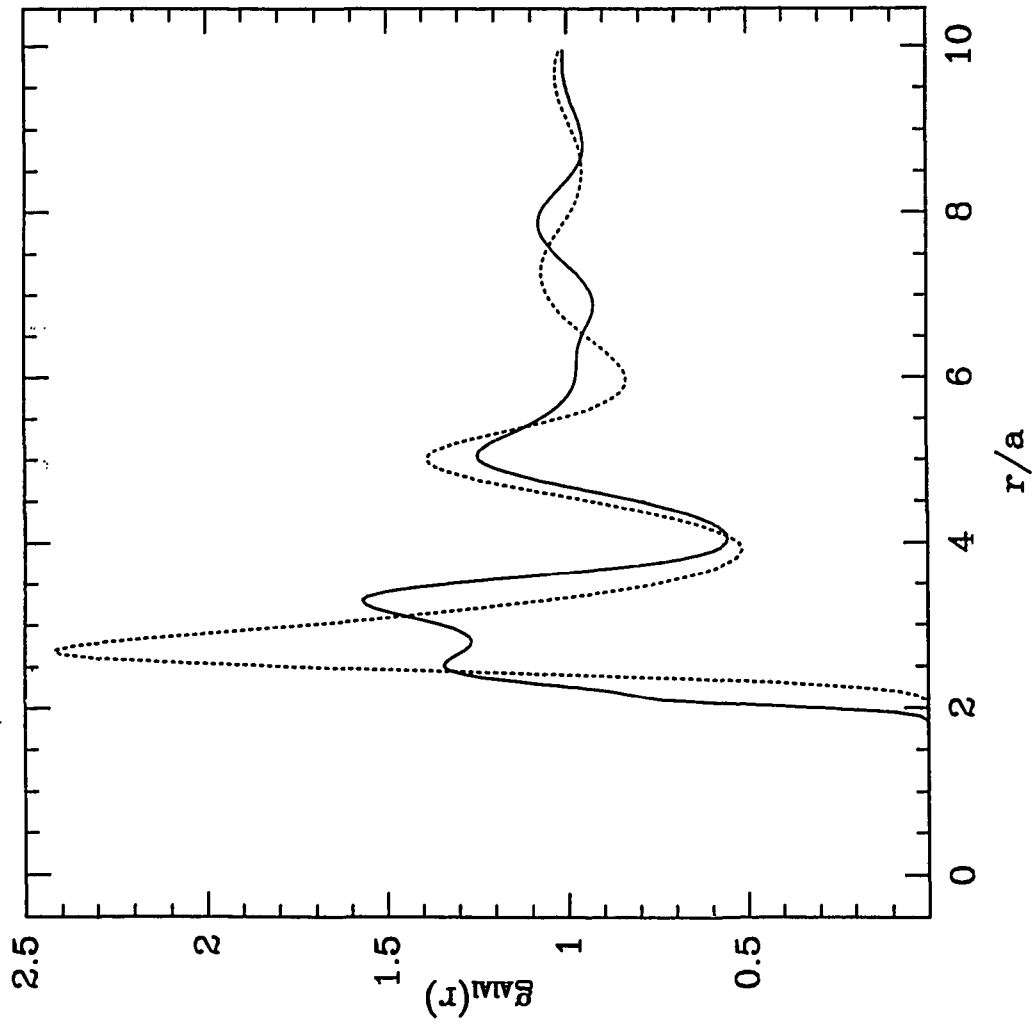


Fig. 4c

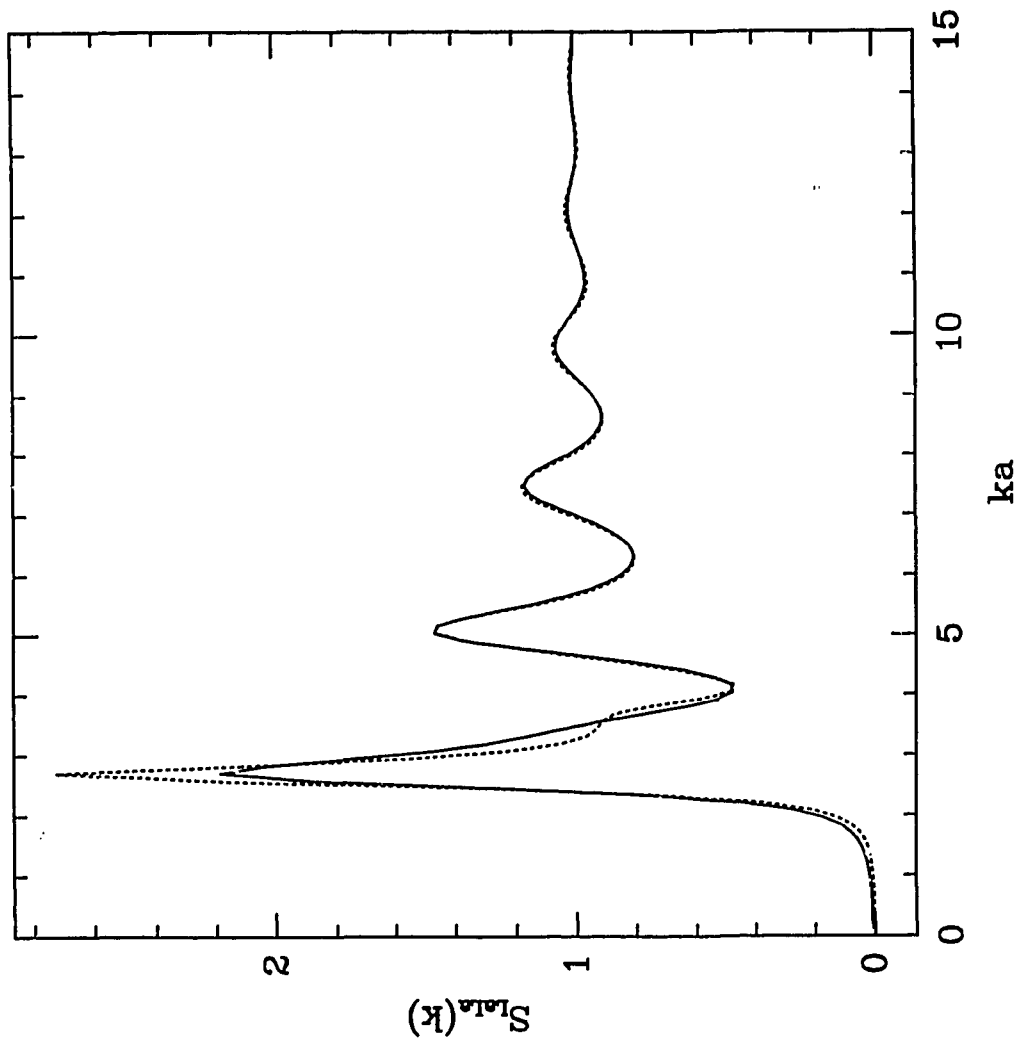


Fig. 5a

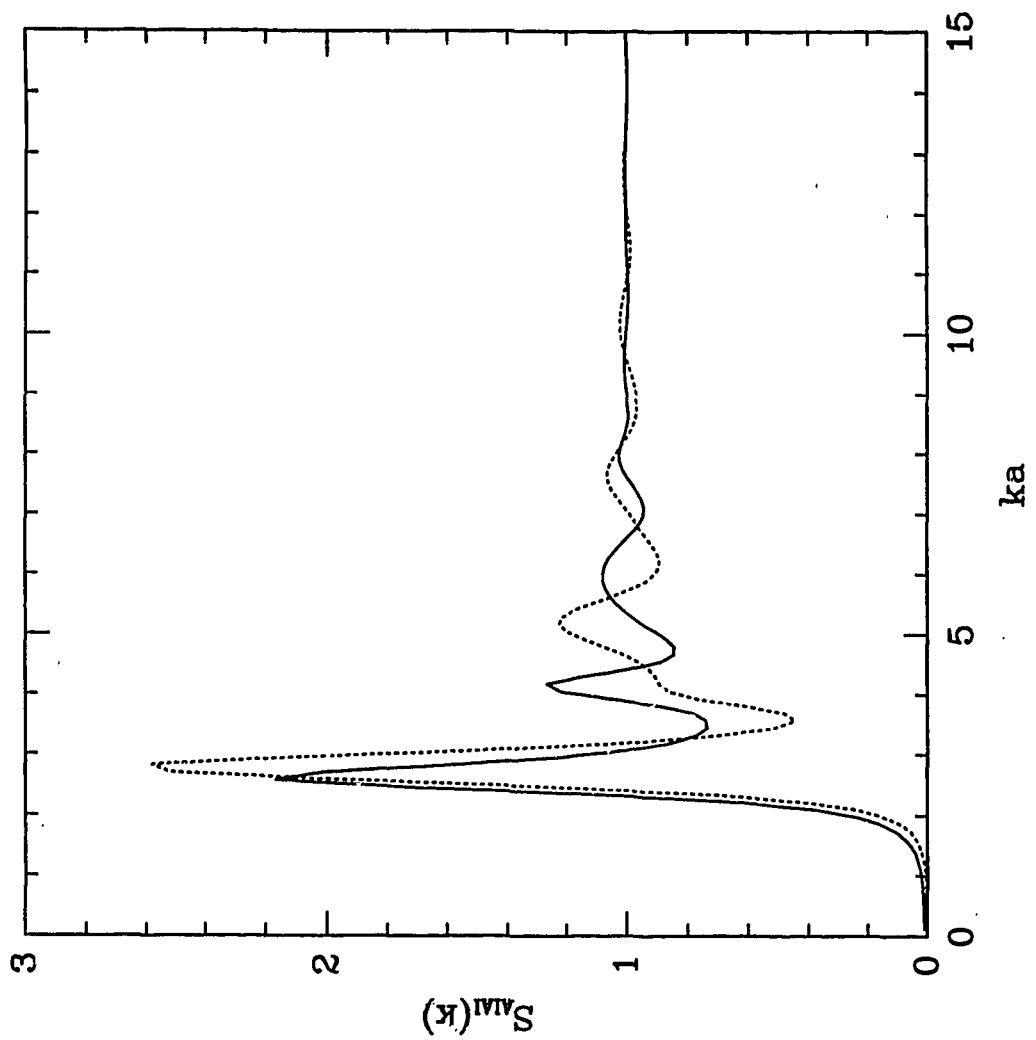


Fig. 5c

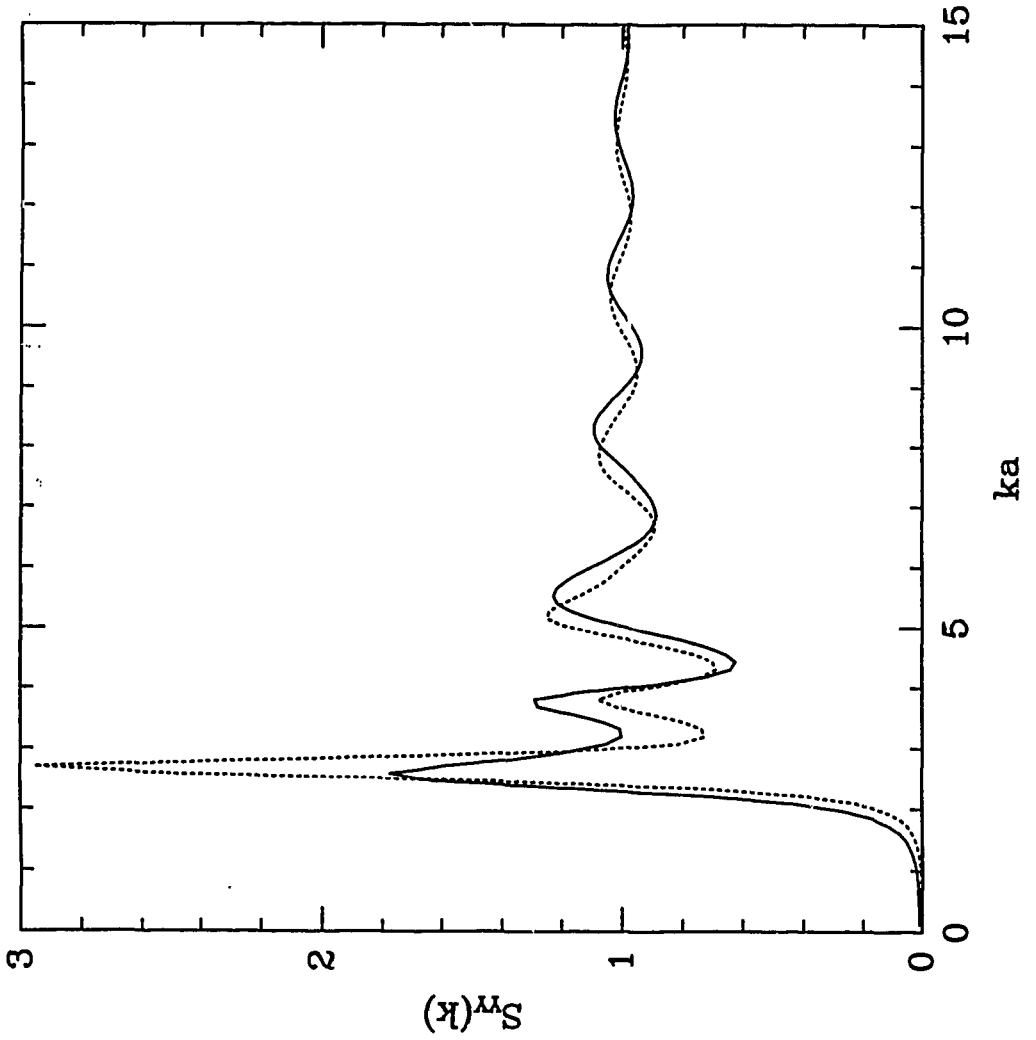


Fig. 5b

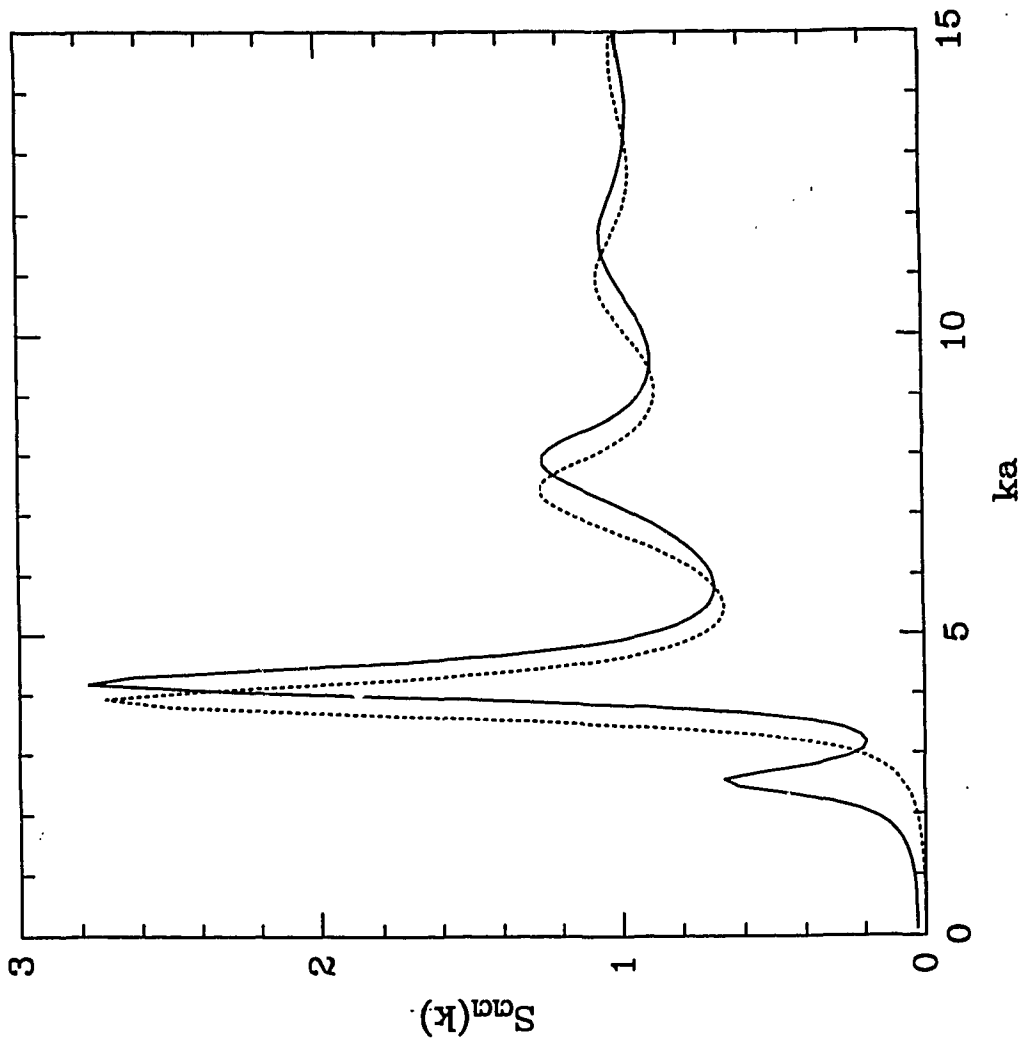


Fig. 6b

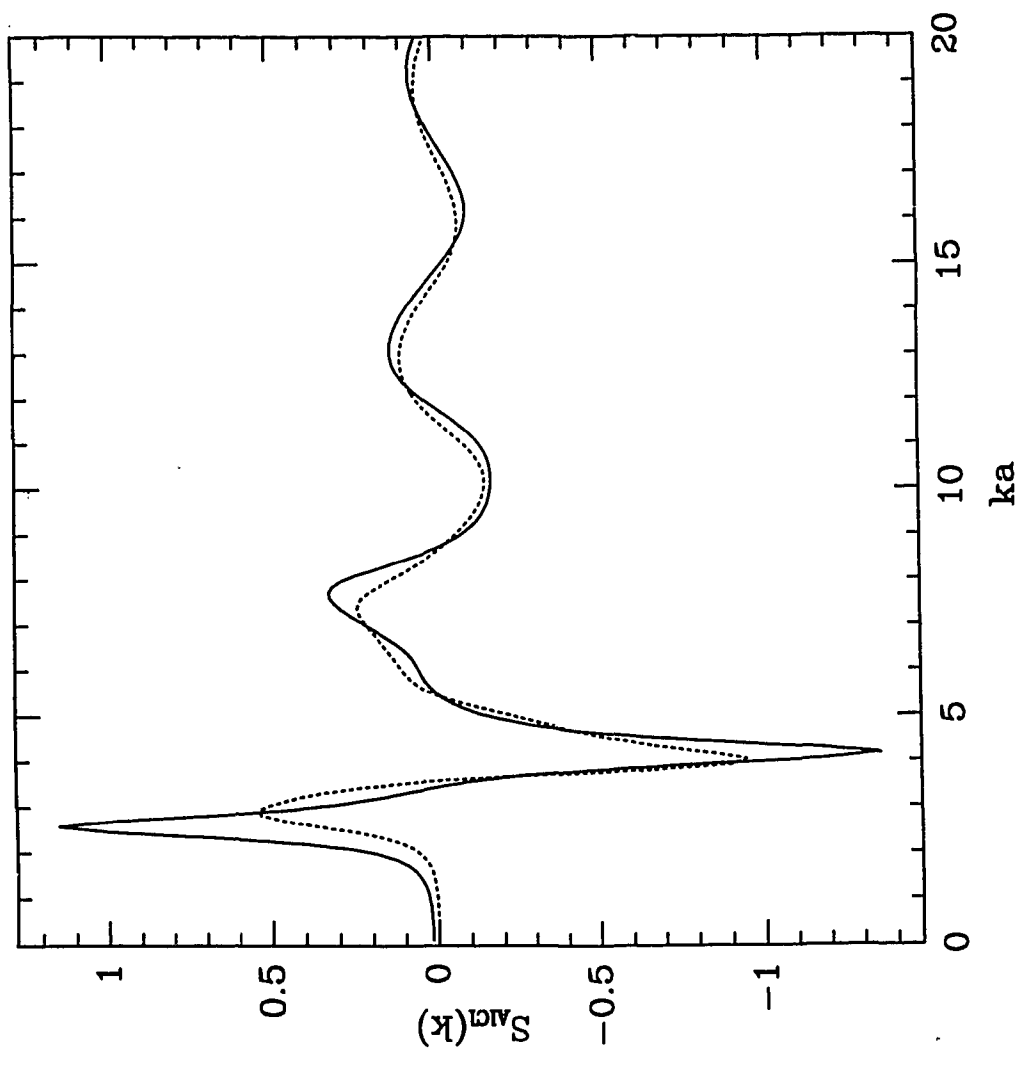


Fig. 6a